

The effects of BMMSC treatment on lung degeneration in elderly macaques

**Yu-kun YANG^{^1, 2, 3, 5}, Guang-ping RUAN^{^1, 2, 3}, Ye LI^{1, 2, 3}, Yan-ying WANG^{1, 2, 3},
Chuan TIAN^{1, 2, 3}, Qiang WANG^{1, 2, 3}, Huanyu HE^{1, 2, 3, 5}, Gaohong ZHU⁴, Dong
Fang⁴, Mao WANG⁵, Xiang-qing ZHU^{*1, 2, 3}, Xing-hua PAN^{*1, 2, 3}**

Affiliations:

**¹ Kunming Key Laboratory of Stem Cell and Regenerative Medicine, 920th Hospital of the
PLA Joint Logistics Support Force, Kunming, Yunnan Province, China, 650032**

**² Stem Cells and Immune Cells Biomedical Techniques Integrated Engineering Laboratory of
State and Regions, Kunming, Yunnan Province, China**

**³ Cell Therapy Technology Transfer Medical Key Laboratory of Yunnan Province, Kunming,
Yunnan Province, China**

**⁴ Department of Nuclear Medicine, the First Affiliated Hospital of Kunming Medical
University, Kunming, Yunnan Province, China**

⁵ Kunming Medical University, Kunming, Yunnan Province, China

[^]these authors contributed equally to this work

***Correspondence to: Xiang-qing ZHU, Email: qing1021zhu@163.com, Xing-hua PAN,
Email: xinghuapan@aliyun.com**

Abstract

Age-related degeneration of lung tissues increases the risk of lung injury and exacerbates lung disease. It is also the main risk factor for chronic lung diseases (such as COPD, idiopathic pulmonary fibrosis, cancer, etc.). Here, we performed systematic screening, evaluation of elderly macaque model. A senile multiple organ dysfunction model was used to explore whether BMMSC could improve degeneration of lung tissues in an elderly macaque model. Using model evaluation tests, we found that the average alveolar area, Mean linear intercept (MLI) and fibrosis area in the elderly macaque models were significantly larger than in young rhesus monkeys ($P < 0.05$), and

the capillary density around the alveoli was significantly lower than in young macaque models ($P < 0.05$). Intravenous infusion of BMMSC reduced the degree of pulmonary fibrosis in elderly macaque, increased the density of capillaries around the alveoli ($P < 0.05$), and the number of type II alveolar epithelium in elderly macaque ($P < 0.05$). BMMSC infusion reduced lung tissue ROS level, systemic and lung tissue inflammation level and Treg cell ratio in elderly macaque model ($P < 0.05$). Indirect co-cultivation revealed that BMMSC reduced the expression of senescence-related genes, ROS levels, apoptosis rate of aging type II alveolar epithelial cells (A549 cells) and promoted their proliferation ($P < 0.05$).

Key words: BMMSC, lung degeneration, type II alveolar epithelial cells, macaque

Introduction

The aging population in China is one of the main problems currently being faced. By 2050, it is expected that the percentage of the population aged 65 years or above will represent about 20% of the population. With age, the respiratory system undergoes various structural changes including a gradual increase in aging-related deterioration in lung tissue, alveolar enlargement, alveolar wall destruction, reduced gas exchange surface area, increased airway obstruction or occlusion, decreased pulmonary vascular density, increased collagen deposition and decreased elastin, etc ^[1-3]. Immune system disorders, including non-specific inflammation and suppressed immune responses, etc ^[4], functional changes, such as loss of elastic recoil, increased residual volume and barriers to gas exchange^[1, 5], increases the susceptibility of the lungs to injury among the elderly and development of chronic lung diseases such as COPD, idiopathic pulmonary fibrosis and cancer ^[6]. Therefore, improving and delaying aging-related lung degenerative changes should be investigated.

Mesenchymal stem cells are multipotent stem cells characterized by low immunogenicity, self-renewal ability, and multi-directional differentiation potential.

Because of the significance of immune regulation in anti-apoptosis, angiogenesis, migration, differentiation to target organs, support of the growth and differentiation of local stem cells and progenitor cells, anti-scarring, and chemical gravity have been used in the treatment of various diseases^[7].

Numerous studies have suggested that mesenchymal stem cells can repair lung injury and effectively treat acute and/or chronic lung diseases ^[8-10]. However, the majority of these studies have been performed on rodents, and very few studies on primates exist. Moreover, the efficacy of mesenchymal stem cells has not been extensively studied in age-related lung tissue degeneration.

Macaque is one of the most popular non-human primates, known to possess many biological characteristics similar to humans. As a model organism, the macaque is physiologically similar to humans, their genomes have a 93% average sequence identity with humans, hence serve as an ideal model to studies of human health and disease.

Besides, macaques as a model animal, have numerous advantages including controllability of environmental factors, ease of scale, and it is widely used in basic and applied research in biomedicine ^[11, 12].

In our previous studies, we reported the correlation between aging and bone marrow mesenchymal stem cells in macaque as well as its anti-aging ability in 293T cells *in vitro* ^[13]. Therefore, in this study, macaque was used as the experimental animal to determine the effects of bone marrow mesenchymal stem cell(BMMSC) on age-related degeneration both *in vivo* and *in vitro*.

Materials and Methods

Animal and cell sources

The macaques used in this experiment were obtained from the Kunming Institute of Zoology of Chinese Academy of Sciences [SCXK (Yunnan) K2017-0003]. In total, we used 33 female animals, aged between 2-26 years old and weighing 2.2-12 kg. The

animals were housed in the Experimental Animal Center of the 920th Hospital of the Chinese People's Liberation Army Joint Logistics Support Force, experimental animal license number: SYXK (Military) 2017-0051, the research program was passed by the experimental animal council of the 920th Hospital of Joint Logistics Support Force

The bone marrow used in our experiments was self-made; A549 cells were purchased from the Wuhan Sevier company with identification certificate, and were subcultured and preserved in liquid nitrogen in our laboratory.

Main Reagents and antibodies

FBS and penicillin - streptomycin solution were purchased from Servicebio; DMEM / F12 media were purchased from Hyclone; 0.25% pancreatin-0.04% EDTA were purchased from Invitrogen; 30% hydrogen peroxide solution was purchased from Solarbio; Cell senescence β -galactosidase staining kit, apoptosis detection kit, active oxygen detection kit, cell cycle and apoptosis detection kit were purchased from Beyotime Biotechnology; Anti-proSP-C antibody was purchased from Sigma; Mouse anti-human CD45, mouse anti-human CD73, Cell staining buffer, True-Nuclear Transcription Factor Buffer Set, Alexa Fluor® 647 anti-human FoxP3, FITC anti-human CD4, PE anti-human CD25 antibody, PE Mouse IgG1 κ Isotype Ctrl and Alexa Fluor® 647 Mouse IgG1 κ Isotype Ctrl were purchased from Biolegend; Monkey interleukin 1 β (IL-1 β) ELISA kit, monkey interleukin-17A (IL-17A) ELISA kit, human tumor necrosis factor alpha (TNF- α) ELISA kit were purchased from Meimian; Fluorescent secondary antibody HRP, fluorescent secondary antibody CY3 and primers were purchased from Servicebio; GoScript™ Reverse Transcription System, GoTaq® qPCR Master Mix were purchased from Promega Corporation; TNF alpha Antibody, IL-10 Antibody and CEBPB Antibody were purchased from Proteintech group; Adipogenic differentiation medium, osteogenic differentiation medium, and chondrogenic differentiation medium were purchased from Guangzhou Saiye Biological Technology Co., Ltd.; ¹⁸F-FDG was provided by the First Affiliated Hospital

of Kunming Medical University

Experimental protocols

Screening and evaluation of senile lung degeneration macaque models

Female macaque aged 22-26 years old were used as the elderly model group, while female young macaque aged 6-8 years old were used as the young control group, with 5 animals in each group. About 5ml of peripheral blood was collected from cynomolgus monkeys, and centrifuged to obtain serum. These sera samples were used for ELISA tests to quantify TNF- α and IL-1 β levels. Next, the macaque were anesthetized with 3% pentobarbital sodium 5ml / kg, and sacrificed to obtain lung tissues. Some the tissue samples were used for size, morphological and texture analysis, while the remaining were subjected to HE staining. The degree of pulmonary fibrosis in the two groups was determined by Masson staining. Capillary density was examined by immunohistochemistry. ROS staining tests were performed to compare oxidative stress levels between the two groups. Western blot was performed to quantify the expression levels of IL-1 β , TNF- α and IL-6 in lung tissues, as indicators of inflammation levels.

Preparation and identification of macaque bone marrow mesenchymal stem cells

Two 2-3 years old macaques randomly were selected and anesthetized with intramuscular injection of 3% pentobarbital sodium at 1 ml / kg. They were placed on the operating table in a supine position, and bone marrow aspiration was performed above and behind the anterior superior iliac spine. This was done using a 20 ml syringe containing 5 ml of heparin sodium saline (100 U / ml). Briefly, 5 ml of bone marrow were drawn. Thereafter, red blood cells were removed by addition of 0.38% ammonium chloride to the bone marrow samples, followed by centrifugation to prepare single cells. The cells were resuspended in DMEM / F12 medium containing 20% fetal bovine serum and seeded in a 175 cm² cell flask. The medium was changed 5 days later, and at intervals of 3 days thereafter. When the adherent cells reached became 80% confluent, they were passaged. The P3 generation of cells was used to perform morphological examination and characterization of growth patterns. Expression of surface antigens

CD29, CD45, CD73, CD90 and CD184 was determined by flow cytometry. and induce their differentiation into osteocytes, chondrocytes, fat cells by In vitro special induction medium to verify their differentiation ability. The proliferation ability of cells was determined by CCK8 assay.

Observation of the histological structure of lung tissues of macaque after BMMSC infusion

Changes in lungs were imaged with PET-CT before BMMSC treatment and at 90 days and 180 days after treatment. At 180 days after BMMSC treatment, macaque were killed by anesthesia, lung tissue was collected, observed and photographed. The right lung was excised, fixed with 4% paraformaldehyde solution, embedded in paraffin and sectioned. The tissue sections were used for HE staining, Masson staining. Immunohistochemistry was used to observed lung tissue structure (i.e., the change of general lung anatomy, alveolar size, inflammation, alveolar septum thickness, pigmentation, pulmonary fibrosis, and changes in capillaries around the alveoli).

Analysis of the effect of BMMSC on type II alveolar epithelial cells

A549 cells were placed in a complete medium containing 200 μ mol / L, 400 μ mol / L, 600 μ mol / L, 800 μ mol / L, 1000 μ mol / L, 1200 μ mol / L hydrogen peroxide. PCR assay was performed on the cells to determine expression of P53 gene while β -galactosidase staining was carried out to determine the optimal concentration of hydrogen peroxide. The expression of *TERT*, *TCABI*, *P53*, *P21* was quantified by RT-PCR. The expression of these genes reflect the level of senescence of A549 cells at the specific hydrogen peroxide concentration. Once a senescence model of type II alveolar epithelial cell was established, the cells were co-cultured with BMMSC in transwell chambers. Thereafter, the expression of *P53*, *P21*, *TCABI* was determined using RT-PCR while rate of apoptosis was determined by flow cytometry. ROS levels and cell cycle progression were compared between the model and treatment group. Immunohistochemistry was performed to detect proSPC as markers of type II alveolar epithelial cells, quantify the number and proliferation rate of type II alveolar epithelial cells in lung tissue.

Analysis of the effect of BMMSC treatment on ROS, inflammatory factors and VEGF in elderly macaques

Serum was prepared from the peripheral blood of macaque obtained at 0, 30, 60, and 90 days after BMMSC treatment. The level of inflammatory factors IL-1 β , IL-17A, and TNF- α in the peripheral blood was detected by ELISA. Left lung tissues were used to measure ROS content after BMMSC treatment by ROS staining. The protein level of proinflammatory factors IL-6, TNF- α , IL-1 β and anti-inflammatory factor IL-10 in the lung tissue was detected by Western blot. Expression of VEGF in lung tissue after BMMSC treatment was also determined by Western blot.

Analysis of the effect of BMMSC treatment on the ratio of peripheral blood Treg cells and FOXP3 in lung tissues of elderly macaque

Lymphocytes were isolated from blood samples obtained from the animals at 0, 30, 60, and 90 days after BMMSC treatment. Changes in Treg cell ratio in peripheral blood was detected by flow cytometry; Treg cells were labeled with FOXP3, and the changes in FOXP3 content were analyzed by immunohistochemistry.

Statistical analysis

Statistical analyses were performed using SPSS 21.0 statistical software. Measurement data are expressed as mean \pm standard deviation ($\bar{X} \pm s$). The means of three or more than three groups were analyzed by one-way ANOVA (One-Way ANOVA).

Results

Differences in appearance and lung tissue structure between the young and elderly macaques

Elderly macaques were found to have a dull coat that turned white, especially around the head and face. Besides, their skin was loose and dry, and the face red (Fig. 1).



Fig .1 age-related change in appearance between the young control group and the elderly model group

The lung tissue of the young control group and the elderly model group were soft, butterfly-shaped, flexible, and pale red. However, when compared with the young control group, the lung volume of the elderly model macaque was significantly larger than that of the young control (Fig. 2).

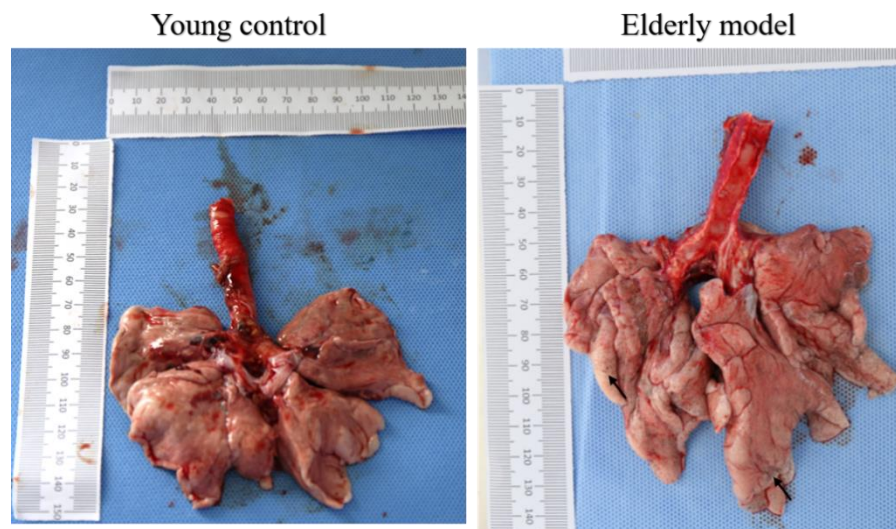


Fig .2 Comparison of lung volume between the young control group and the elderly model group.

The young control group showed clear lung structures, thin and smooth alveolar walls, no thickening of the alveolar space, no exudate, and only a small amount of inflammatory cellular infiltrate around the blood vessels. In the elderly model group, although the alveolar wall thickness was uniform and the alveoli clean, there was no exudate, the alveolar cavity became irregularly enlarged to form the pulmonary bullae

and there was visible pigmentation (as indicated by the black arrow). The elderly model group showed severe inflammation compared with the young control group. The average area and MLI were significantly increased in the elderly model group compared to the young control group (Fig 3), ($P < 0.0001$).

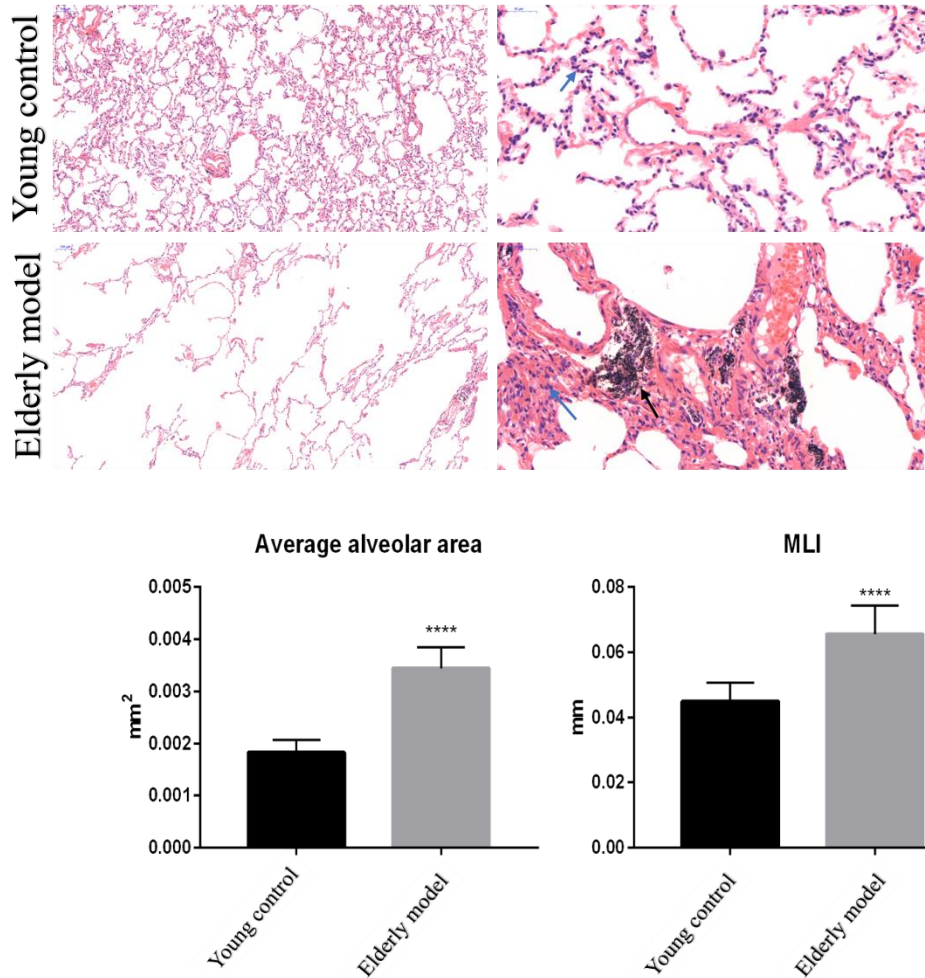


Fig.3 Comparison of the lung tissue structure between the young control group and the elderly model group (n=5, **** $P < 0.0001$ when compared with the young control group)

Masson staining colored the collagen fibers blue. The collagen area in the lungs of the elderly model group was significantly increased, compared with the young control group (Fig .4),($P < 0.01$).

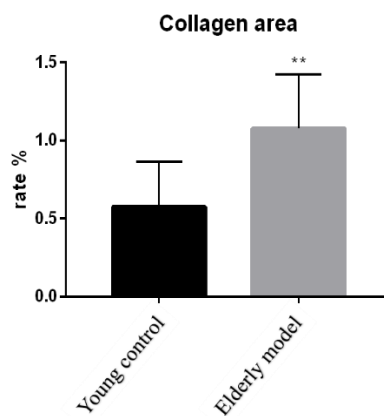
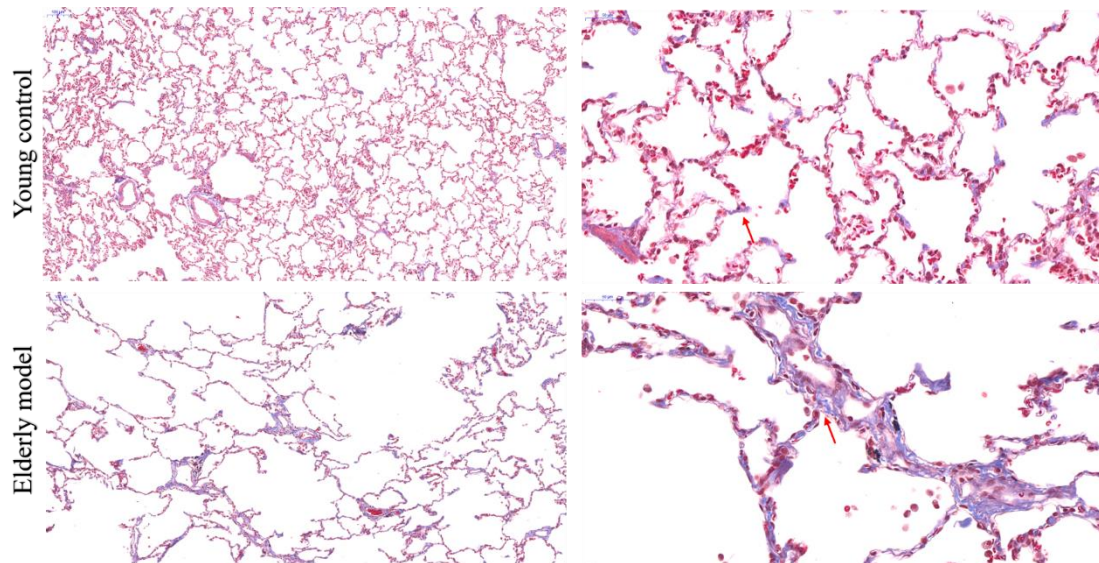


Fig .4 Comparison of the collagen area between the young control group and the elderly model group

(n=5, ** P < 0.01 when compared with the young control group)

Immunohistochemical staining to label the vascular endothelial cells with CD31 revealed that the lung tissue cells nuclear were stained blue, and the surface markers of vascular endothelial cells CD31 were stained brown. In the elderly group, the expression of CD31 in the lungs was significantly reduced compared with the young control group (Fig .5), (P < 0.0001).

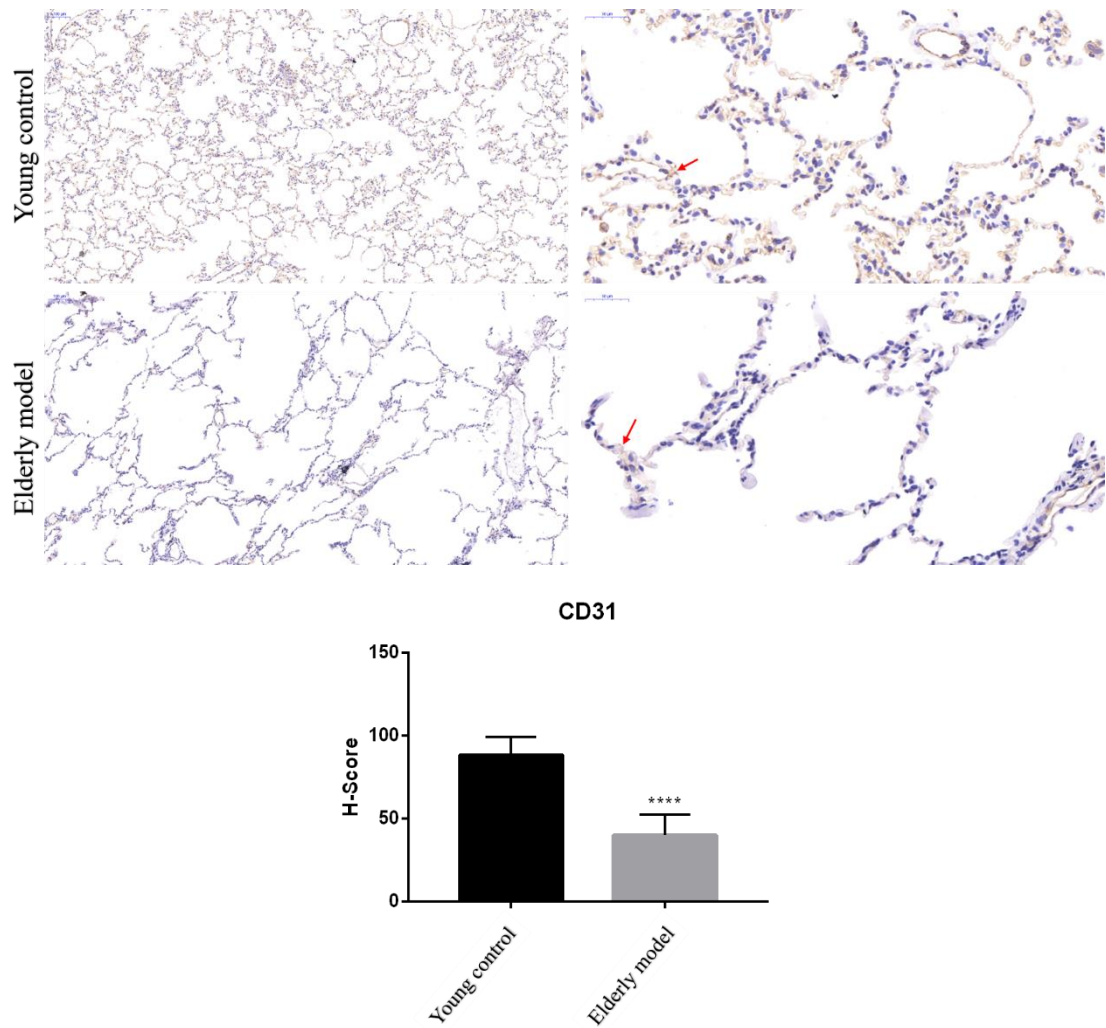


Fig .5 Comparison of CD31 expression around the alveoli between the young control group and the elderly model group(n=5,** P <0.0001 when compared with the young control group)**

Cultivation and identification of BMMSC

Macaque BMMSCs were isolated from bone marrow aspirates and cultured by adherent culture screening. A few fusiform adherent cells were observed under an inverted phase-contrast microscope after 3-4 days. The cell fusion rate had reached about 80% after 9 days. BMMSCs of passage 3 to 5 showed uniform morphology, they grew densely spiral and were isolated (Fig .6A).

To confirm the purity of the cultured cells, the immunophenotypes of the P3 generation of juvenile macaque BMMSC were analyzed by flow cytometry. A panel of surface

antigens was analyzed. The results showed that the BMMSCs were positive for CD29, CD45, CD73, CD90 and CD184 at percentage rates of 96.35 ± 0.62 , 0.16 ± 0.12 , 95.22 ± 0.37 , 96.25 ± 1.71 , 93.53 ± 2.76 , respectively (Fig .6B,Table 1).

Table 1 Flow cytometry analysis of surface antigens

Surface antigen	n	Cell positive rate
CD29	3	96.35 ± 0.62
CD45	3	00.16 ± 0.12
CD73	3	95.22 ± 0.37
CD90	3	96.25 ± 1.71
CD184	3	93.53 ± 2.76

The proliferation assay showed that the BMMSCs took on an “S” shape, the cells remained latent for the first 1-2 days, and entered a logarithmic proliferation phase on 3 to 7 days, where the cells grew vigorously and had the best vitality. On the 8th day, they entered the plateau phase which was characterized by a reduction in proliferation (Fig .6C).

The P3 generation of young macaque BMMSC was used to determine the differentiation ability and proliferation *in vitro*. The duration of the differentiation experiment was 14-21 days. The cells were cultured in osteogenic induction medium and allowed to aggregate, form nodules, and accumulate calcium deposits. Alizarin red stain was used to detect the precipitated calcium deposits which were an indication of differentiation. Intracellular lipid droplets were stained with oil red O, and red-stained lipid droplets were found in the cells. Proteoglycans were stained with Alcian blue and appeared as smears (Fig .6D).

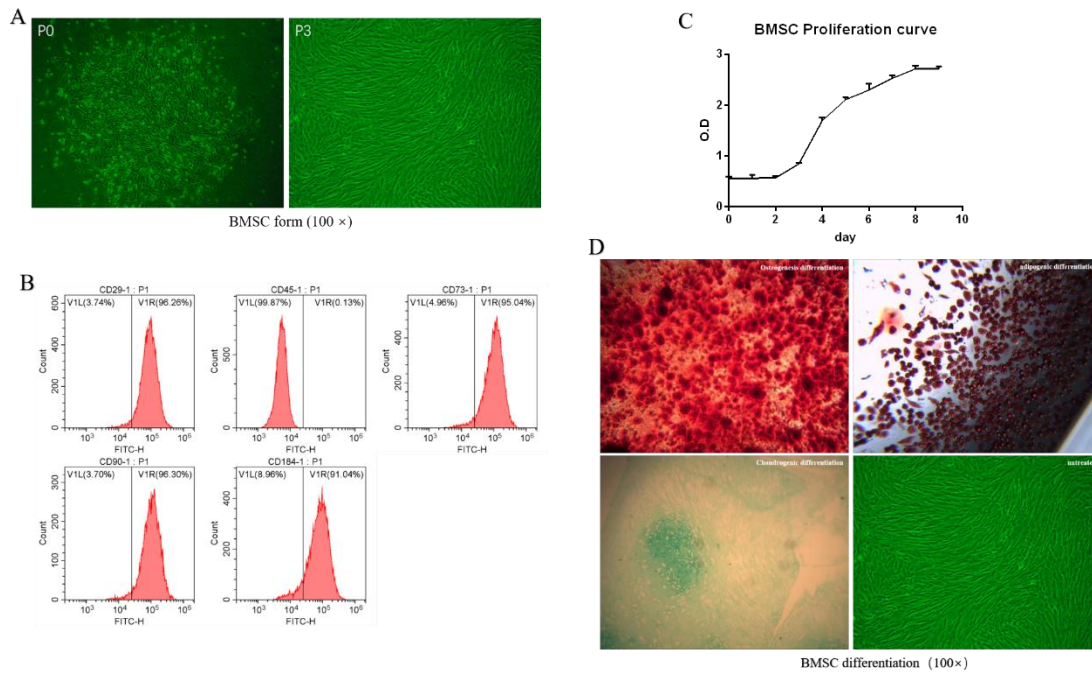


Fig .6 Cultivation and identification of BMMSC a. BMMSC form b. BMMSC flow analysis c. BMMSC proliferation curve d. BMMSC differentiation

The Changes in lung tissue structure after BMMSC treatment

PET-CT examination was performed on the macaques, before treatment, at 90 and 180 days after treatment. The results showed that the texture of the lungs of the macaque before treatment was grid-like, ground-glass opacity, honeycomb-shaped, with the peripheral, subpleural, and lower lung lobes as the main features and emphysema was obvious. The average CT value was significantly decreased before treatment compared with the control group ($P < 0.01$). Before treatment, HRCT showed irregular thickening of the leaflet intervals, and the small blood vessels in the leaflet became obvious due to the thickening of the wall in the treatment group. PET showed that the ^{18}F -FDG uptake quantified as the glucose uptake in the lungs decreased after treatment. At 90 and 180 days, following treatment, CT showed that the lungs' texture was clear, and both hilar were normal. The CT value was higher than before treatment. The average CT values were (685 ± 12.53) and (705 ± 18.53) , respectively (Table 2, Fig .7).

Table 2 Changes in PET-CT in elderly macaque lung after BMMS treatment

	n	CT value	SUV max
Control	5	- (672±12.52)	0.4±0.09
Prior treatment	5	- (853±25.32) \$	0.7±0.06 \$
90 days after treatment	5	- (685±12.53) *	0.5±0.08 *
180 days after treatment	5	- (705±18.53) *	0.3±0.07 **

\$P < 0.05 when compared with the control group, * P < 0.05 when compared with prior treatment, ** P < 0.01 when compared with the prior treatment

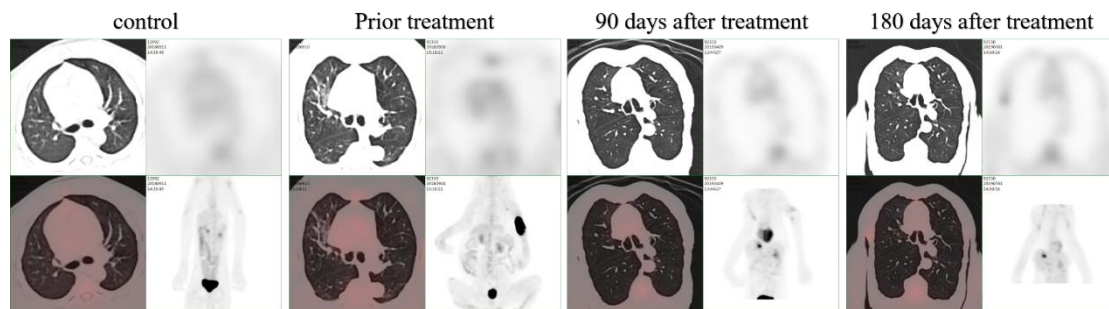


Fig .7 Changes in PET-CT in elderly macaque lung after BMMS treatment

Examination of material from the lung tissue after 180 days of treatment, showed that the lung tissue appeared dark white and red without embolism. However, there were no significant changes observed in both the treatment group compared with the model group (Fig .8).

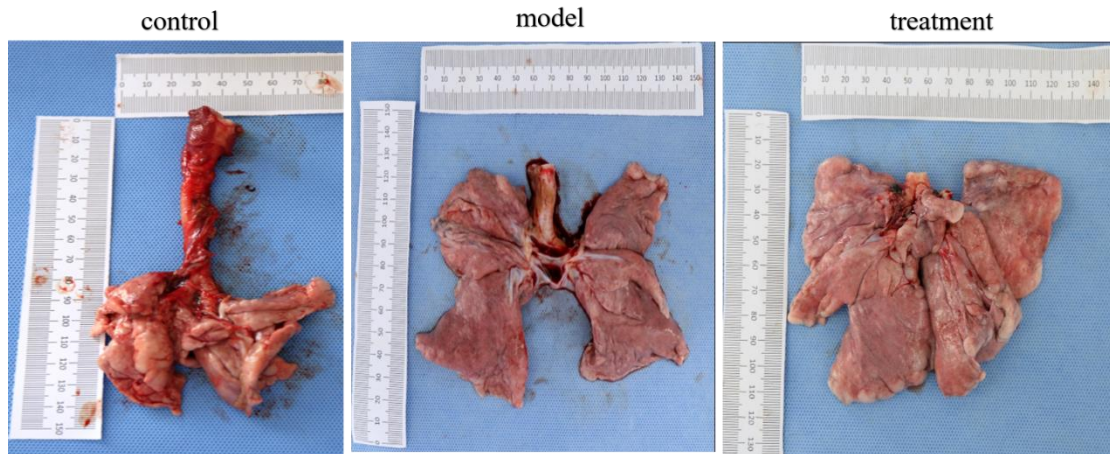


Fig .8 Gross anatomical changes of lung tissue in elderly macaque after BMMSC treatment

HE results showed that the control group had clear lung structures, thin and smooth alveolar walls, no thickening of the alveolar spaces, no exudates, and only a small amount of inflammatory cellular infiltration around the blood vessels. The alveolar cavity showed irregular enlargement and the formation of pulmonary bullae, the alveoli were clean with no exudates seen, a small amount of inflammatory cell infiltration was observed around the blood vessels with pigmentation in the model group macaques and the treatment group macaques. Although the inflammation score was not statistically different in those groups, the treatment group had lower inflammation than the model group. The average alveolar area and alveolar lining interval (MLI) of the model group and the treatment group were both significantly increased compared with the control group, ($P < 0.05$); however, there was no significant difference between the model group and the treatment group (Fig .9), ($P >$

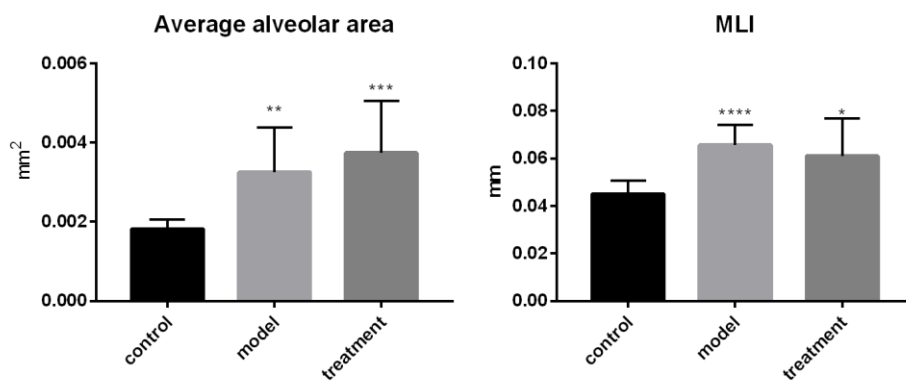
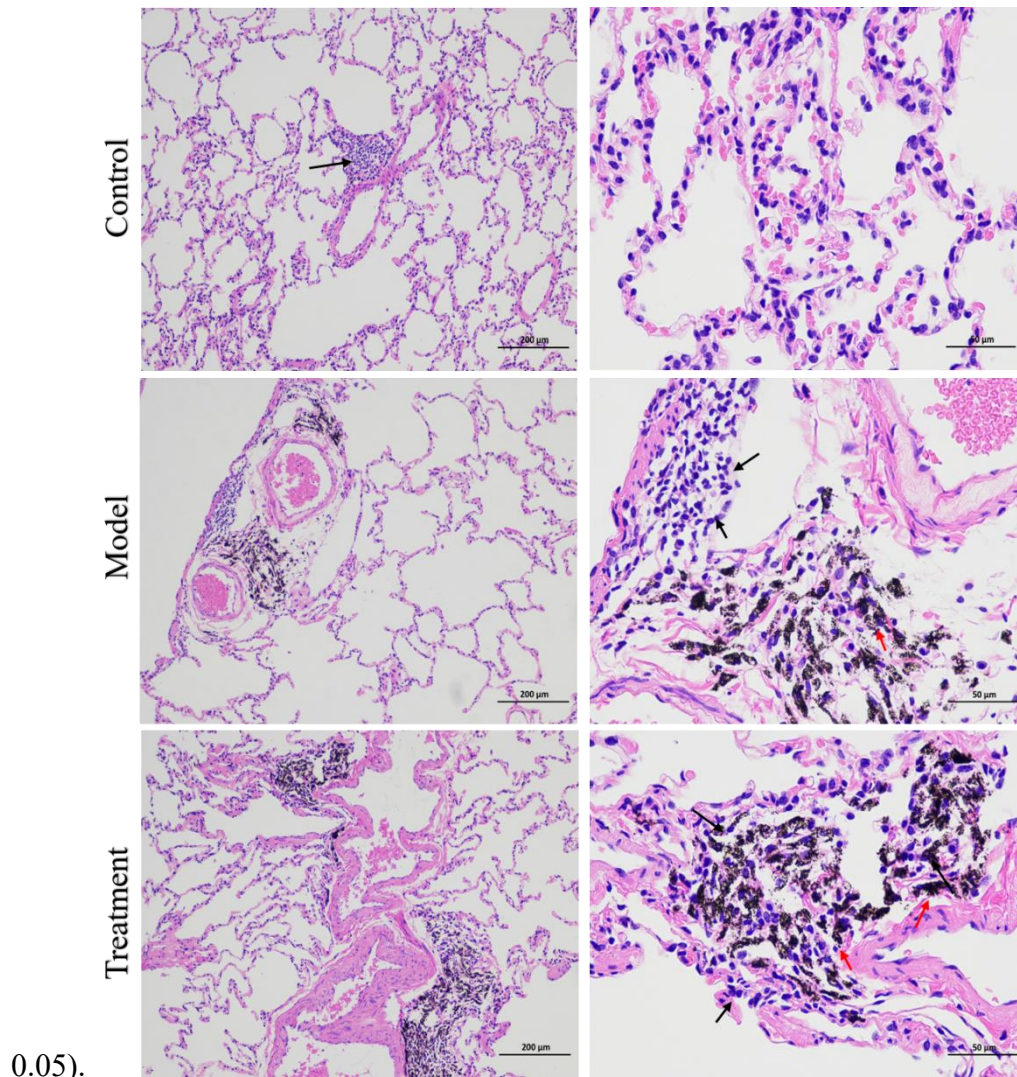


Fig .9 Changes in the structure of lung tissue after BMMSC treatment by HE staining (n=5, * P <0.05 when compared with the control group, ** P <0.01 when compared with the control group, *** P <0.001 when compared with the control group).

Masson staining showed blue collagen. The collagen area of the treatment group was significantly reduced (P <0.05) when compared with the model group (Fig .10).

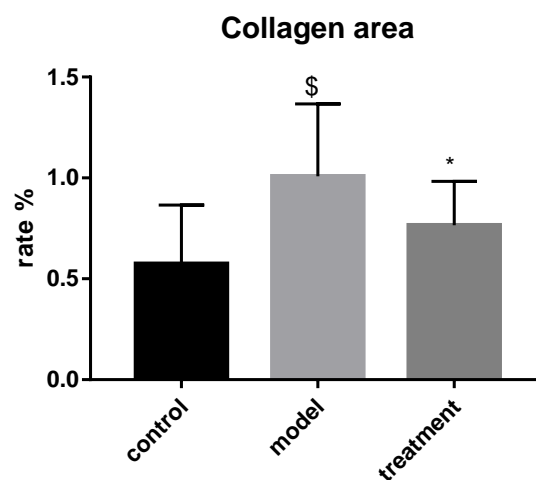
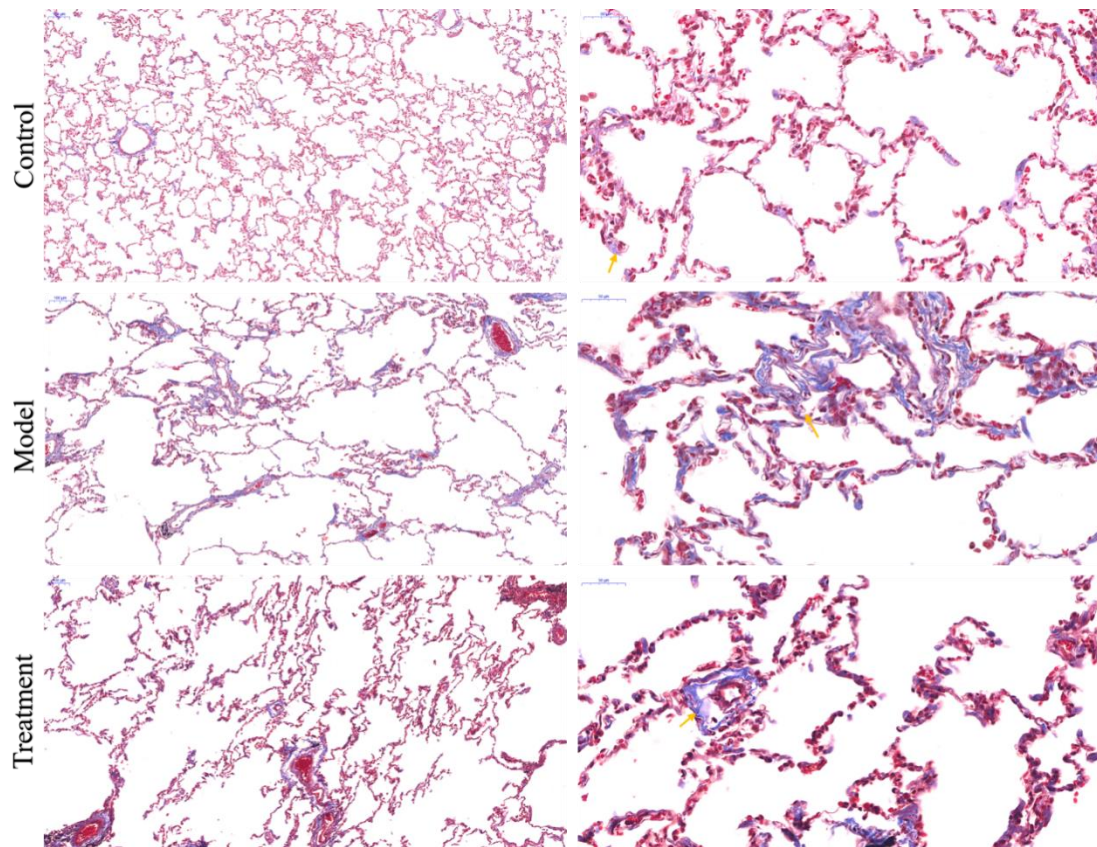


Fig .10 Changes in collagen area in lung tissue after BMMSC treatment (n=5, \$ P<0.05 when compared with the control group, *P<0.05 when compared with the model group).

To determine the changes in capillary density around the alveoli after cell transplantation, immunohistochemistry was performed using CD31 as a marker of vascular endothelial cells. The nucleus stained blue and capillaries with CD31 surface markers were stained brown. The content of CD31 around the alveoli was significantly

increased in the treatment group, compared with the model group (Fig .11), ($P < 0.0001$).

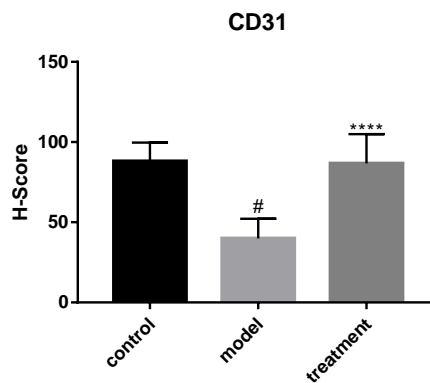
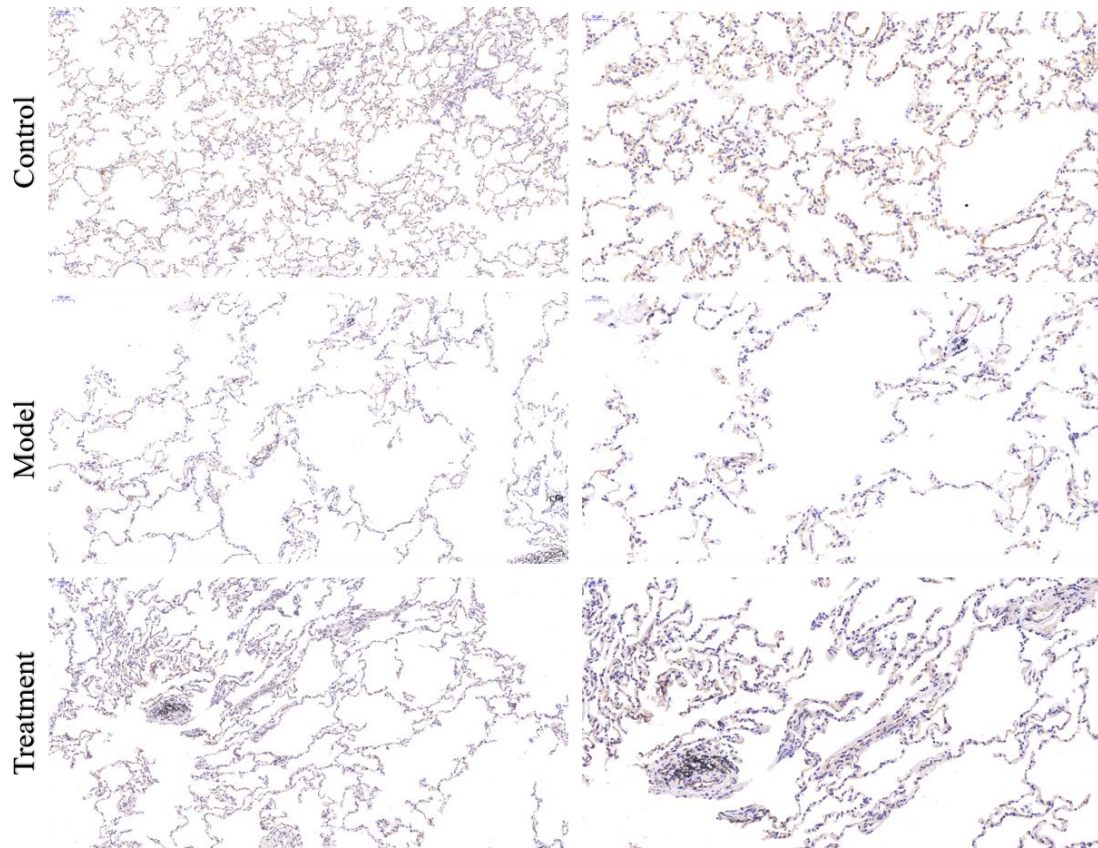


Fig.11 Changes in CD31 surface markers around the alveoli after BMMSC treatment (n=5, # $P < 0.001$ when compared with the control group, **** $P < 0.0001$ when compared with the model group)

Effect of BMMSC on senile type 2 alveolar epithelial cells

Type II alveolar epithelium plays a significant role in lung aging. In the elderly, the quantity and quality of type II alveolar epithelial cells are significantly reduced [14]. In

this study, the effect of BMMSC on lung structure was observed using type II alveolar epithelial cells to explore the specific effect on lung cells. Hydrogen peroxide was used to establish an aging model of A549 cells. Different concentrations of hydrogen peroxide were found to induce different degrees of aging in A549 cells. Following SA- β -gal staining, the aging rate of A549 cells at concentrations of 0mmol/L, 200 μ mol / L, 400 μ mol / L, 600 μ mol / L, 800 μ mol / L were (1.5 \pm 0.5)%, (29 \pm 6)%, 59.33 \pm 5.11)%, (91.66 \pm 7.45)%, (92 \pm 5.33%), respectively. However, 1000 μ mol / L and 1200 μ mol / L were not considered as most of the cells were apoptotic and deformed. There was no significant difference in the rate of aging at concentrations 600 μ mol / L and 800 μ / L (Fig 12),(P > 0.05).

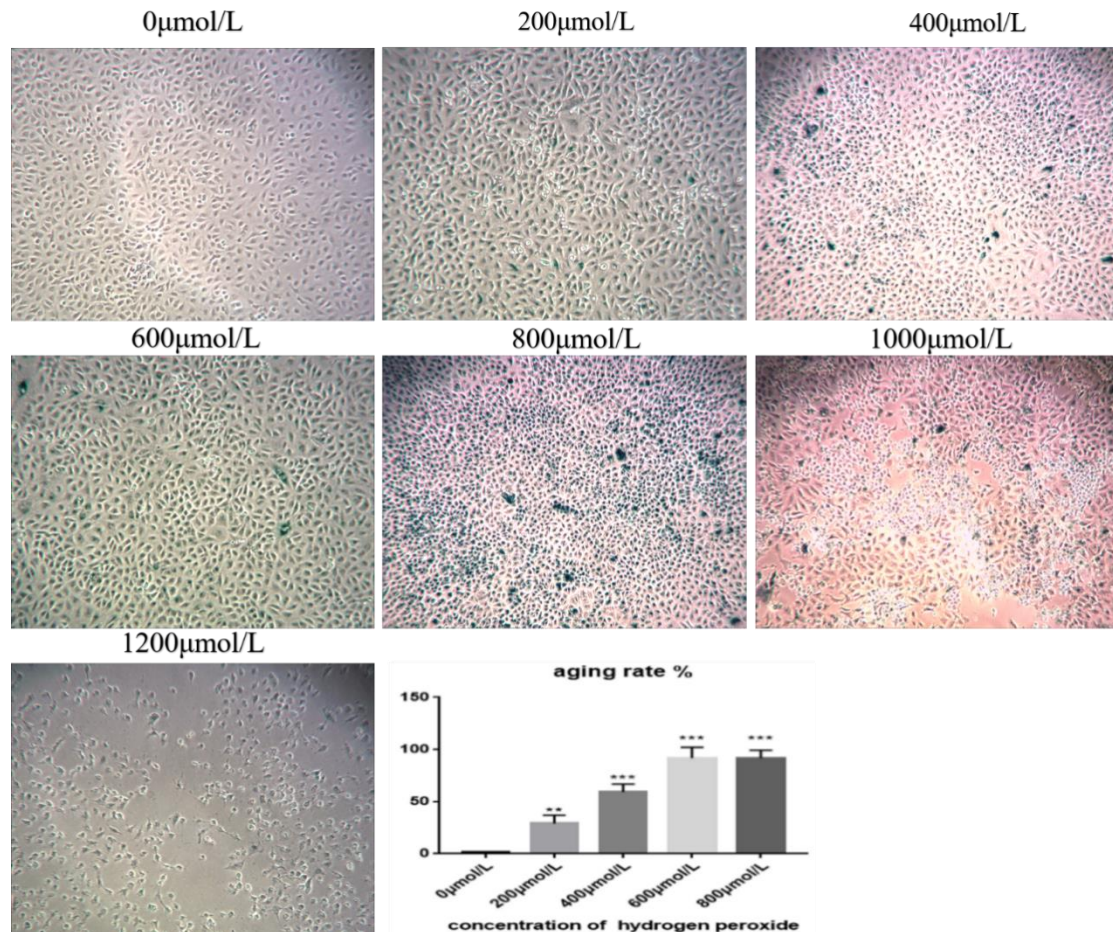


Fig .12 Hydrogen peroxide-induced senescence of A549 cells and β -galactosidase staining (100 \times)(n=3, **P <0.01 when compared with the 0 μ mol/L group, **P <0.001 when compared with the 0 μ mol/L group)**

RT-PCR was used to detect the expression of P53 gene in A549 cells after induction of

aging. The increase in P53 expression was most significant ($P < 0.001$, $P < 0.0001$) at $600\mu\text{mol/L}$, $800\mu\text{mol/L}$ hydrogen peroxide concentration (Fig 13A). Therefore, $600\mu\text{mol/L}$ was chosen as the optimal concentration to induce senescence of A549 cells.

RT-PCR was used to further compare the expression of P53, P21, TERT, TCAB1 before and after induction of aging using hydrogen peroxide at a concentration of $600\mu\text{mol/L}$. At 6h, after induction, the changes in P53 and P21 expression were significantly increased ($P < 0.0001$, $P < 0.001$); however, TERT and TCAB1 were significantly decreased ($P < 0.001$, $P < 0.01$) 6 hours after induction (Fig .13B). At 24h, 48h, and 72h after changing the medium, TCAB1 did not show any significant change ($P > 0.05$), while P21 was significantly increased ($P < 0.0001$). Even though the expression of P53 was significantly decreased after induction ($P < 0.05$), it remained higher than before induction (Fig .13C).

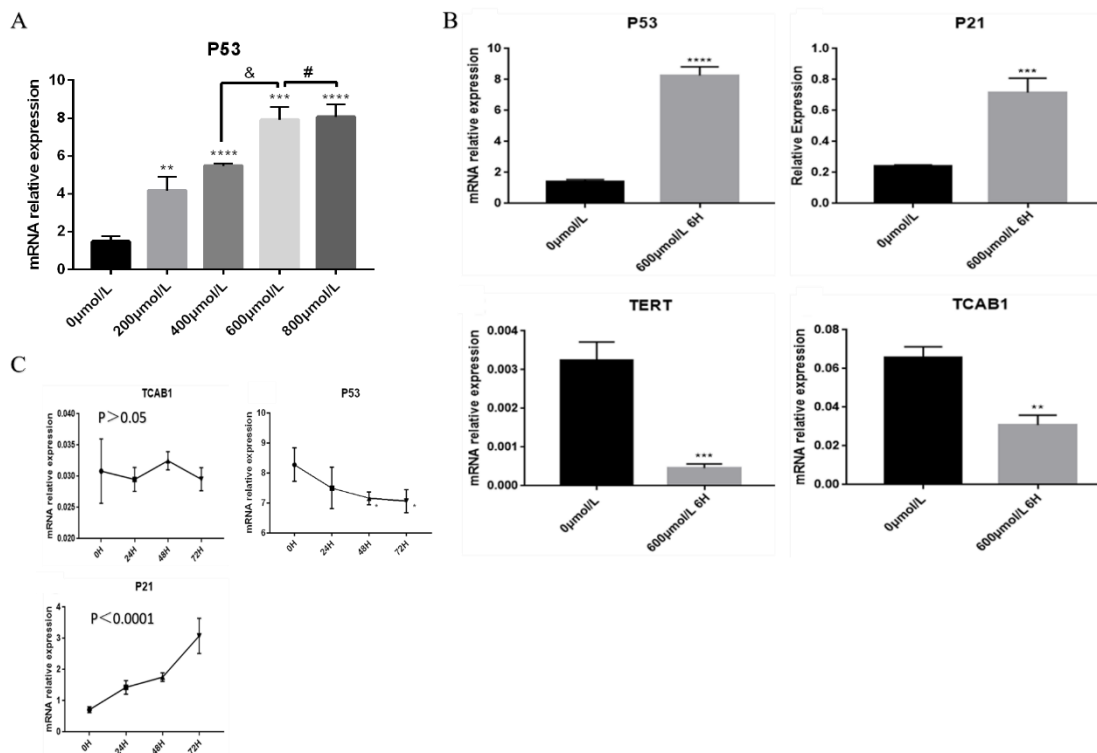


Fig .13 Identification of A549 Aging Model a. qPCR P53 expression After induction($n=3$, $\&P < 0.01$, $\#P > 0.05$, $**P < 0.01$ when compared with the $0\mu\text{mol/L}$ group, $***P < 0.001$ when compared with the $0\mu\text{mol/L}$ group, $****P < 0.0001$ when compared with the $0\mu\text{mol/L}$ group) b. qPCR validation confirming the aging characteristics of

A549 cells aging model (n=3, **P<0.01 when compared with the 0 μ mol/L group, ***P<0.001 when compared with the 0 μ mol/L group, **** P<0.01 when compared with the 0 μ mol/L group) c. qPCR validation confirming the aging stability of the A549 cells aging model (n=3, *P<0.05 when compared with the 0h group)

Following the indirect co-culture of A549 cells aging model with BMMSC for 48H, the lower layer of A549 cell was collected to explore the effect of BMMSC on the A549 aging model by RT-PCR. The expression levels of P53 and P21 were found to be significantly decreased (P <0.001, P <0.01) in the treatment group compared with the model group. However, the expression level of TCAB1 increased significantly (P <0.05) (Fig .14A).

The ROS level, apoptosis ratio, and cell cycle of A549 cells were detected by flow cytometry after indirect co-culture. The ROS level and apoptosis ratio of the treatment group were found to be significantly reduced compared with the model group (Fig .14B, Fig .14C), (P < 0.0001, P <0.001). Proliferation in the treatment group accelerated to the G2 phase (Fig .14D), (P <0.01).

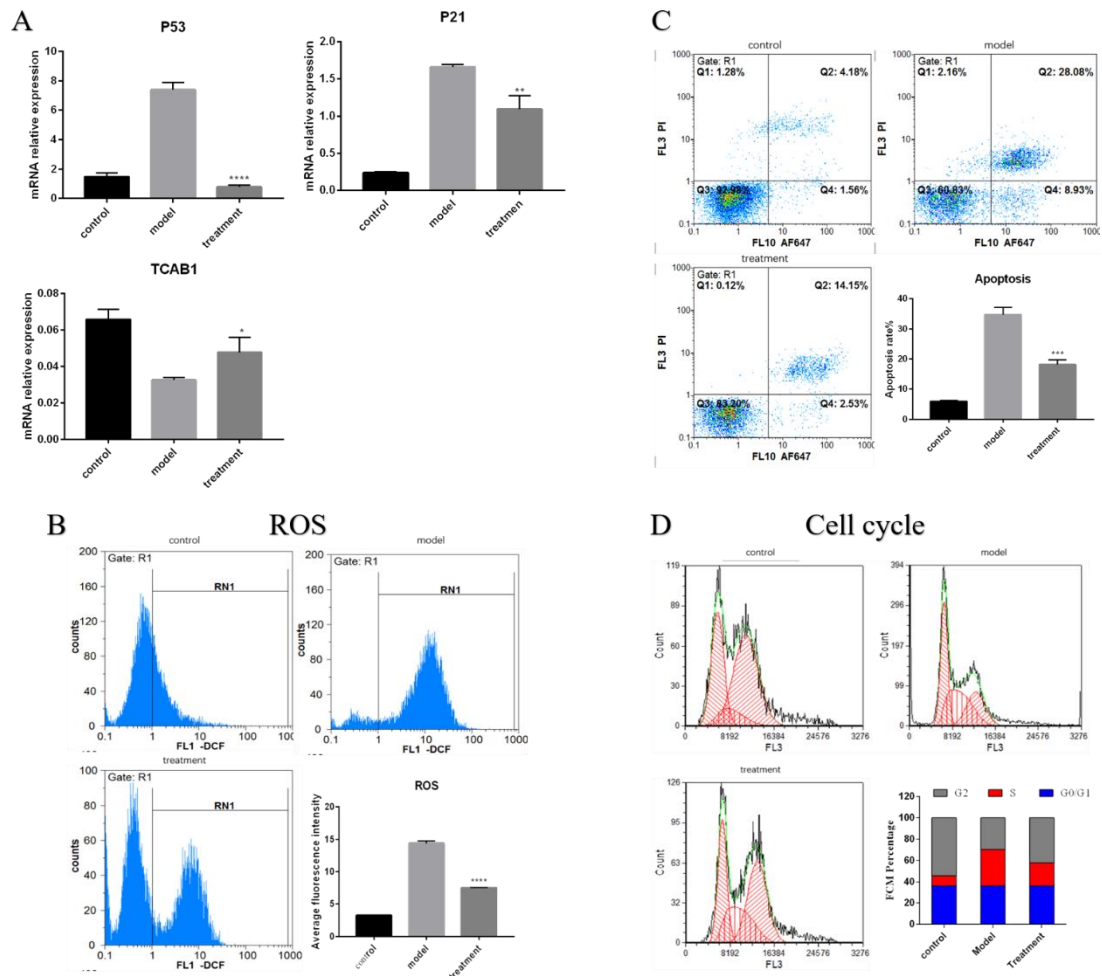


Fig. 14 Effects of BMMSC on the aging model of type II alveolar epithelial cells **a.** qPCR detection of aging-related gene expression after co-culture (n=3,* P<0.05 when compared with the model group, ** P<0.01 when compared with the model group, ***P<0.0001 when compared with the model group) **b.** Changes in cell ROS level after co-culture (n=3,***P<0.001 when compared with the model group, ****P<0.0001 when compared with the model group) **c.** Changes in cell apoptosis rate after co-culture (n=3,***P<0.001 compared with the model group, ****P<0.0001 compared with the model group) **d.** Changes in cell proliferation (n=3)

In vitro experiments, revealed the effects of BMMSC on the aging of the A549 cell model. To verify these effects in vivo, proSPC was used as a marker for type II alveolar epithelial cells. The results showed that type II alveolar epithelial cells were round or oval and scattered in the alveolar wall. The number of type II alveolar epithelial cells in the model group was significantly reduced compared with the control group (P <0.001). However, in the treatment group, typeII alveolar epithelial

cells were significantly increased compared with the model group (Fig .15),(P < 0.01).

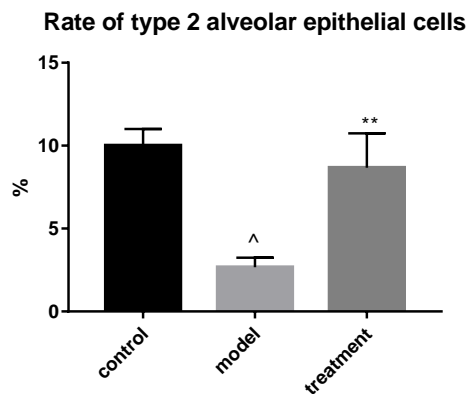
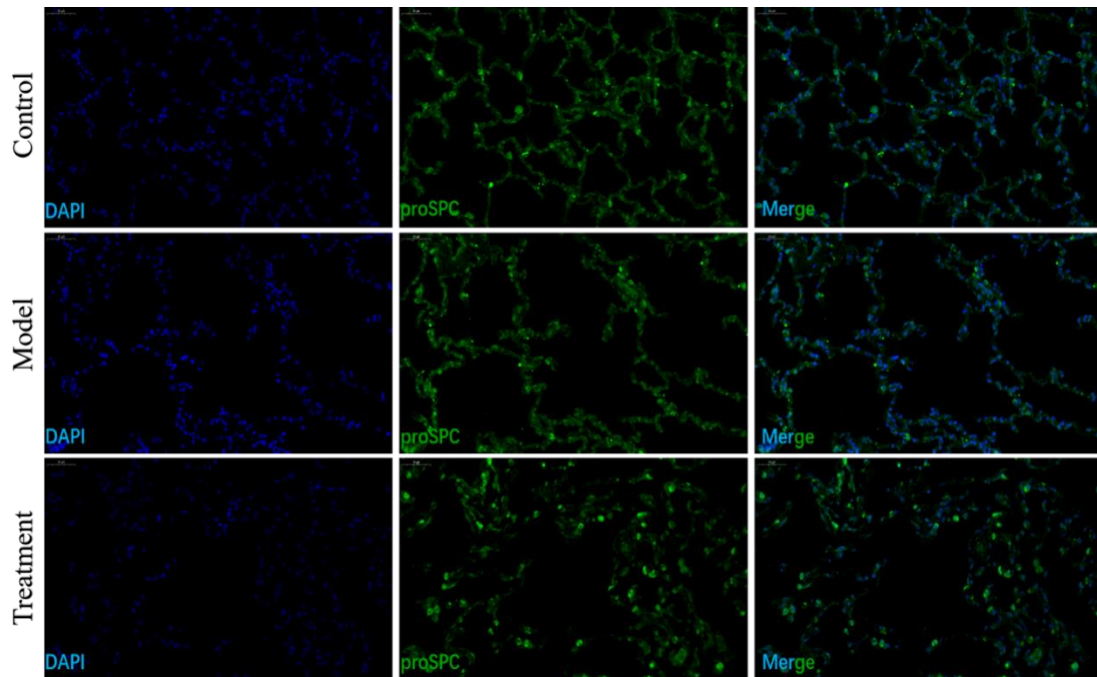


Fig .15 Effect of BMMSC on the number of type II alveolar epithelial cells in the lung tissue
(n=5,**P<0.01 when compared with the model group, ^P<0.001 compared with the control group)

Changes in VEGF expression level in lung tissue

There were observed changes in the density of capillaries around the alveoli, hence there was a need to check on the level of VEGF in the lungs. Western blot analysis of the lung tissue showed that the VEGF in the model group decreased significantly compared with the control group (P <0.05). Besides, after BMMSC treatment, the

VEGF level in the treatment group was significantly higher compared with the model group (Fig .16) (P <0.05).

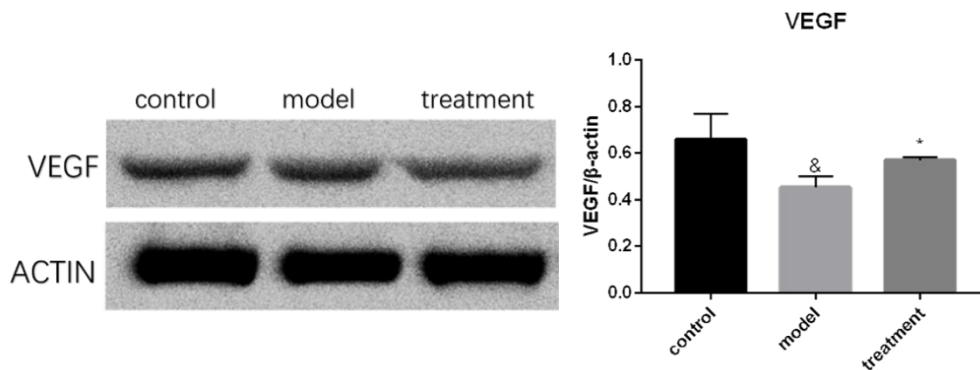


Fig .16 Changes in VEGF level in the lung tissue after BMMSC treatment (n=5, &P <0.05 compared with the control group, *P<0.05 compared with the model group)

Changes in the level of ROS and inflammatory factors after BMMSC treatment

Extensive experiments in a wide range of organisms from yeast to primates have revealed that the nine hallmarks of aging are stem cell failure, changes in intercellular communication, genomic instability and telomere wear, epigenetic changes, loss of protein homeostasis, nutrition changes, mitochondrial dysfunction and cellular senescence [15]. There are still many unresolved issues on the main causes and impacts of these events. However, emerging research suggests that the causes and commonalities of these events are related to the immune system. Inflammatory aging is characterized by elevated levels of immune cell infiltration and elevated levels of pro-inflammatory cytokines and chemokines in the tissue microenvironment and circulatory system [15]. Under normal physiological conditions, ROS in the cells is constantly generated and eliminated. Therefore, maintaining appropriate levels of ROS in the cells plays an important role in the stability of cell functions. However, in the state of aging, the level of ROS may also be elevated due to mitochondrial stress and damage and persistent inflammation [16]. High levels of ROS not only increase damage to the cells but also stimulates immune cells to produce more pro-inflammatory factors to form a vicious circle [17]. The immune regulation and damage repair functions of mesenchymal stem cells are very critical. Studies have reported that MSCs control

inflammation and ROS production through paracrine and mitochondrial transfer between MSCs and aging cells [18, 19]. Therefore, this study proposed that mesenchymal stem cells altered inflammation and ROS levels in elderly macaques thus affecting lung degeneration. The frozen section of lung tissue was used to detect the level of ROS. Using the inverted fluorescent microscope, the lung cells' nucleus was stained blue, and the red fluorescence was distributed in the cytoplasm. Compared with the model group, the ROS level of the treatment group was significantly reduced (Fig .17),(P <0.01).

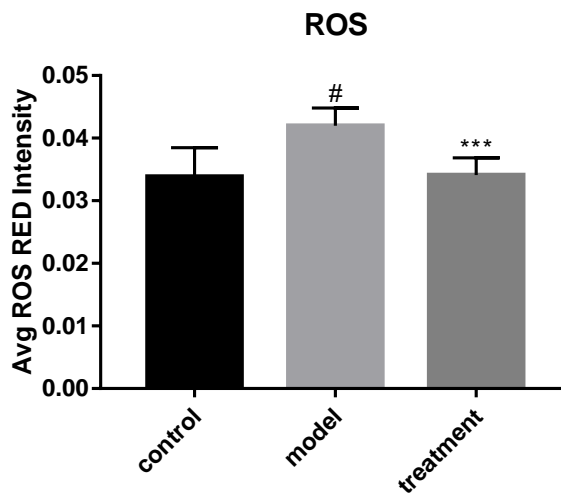
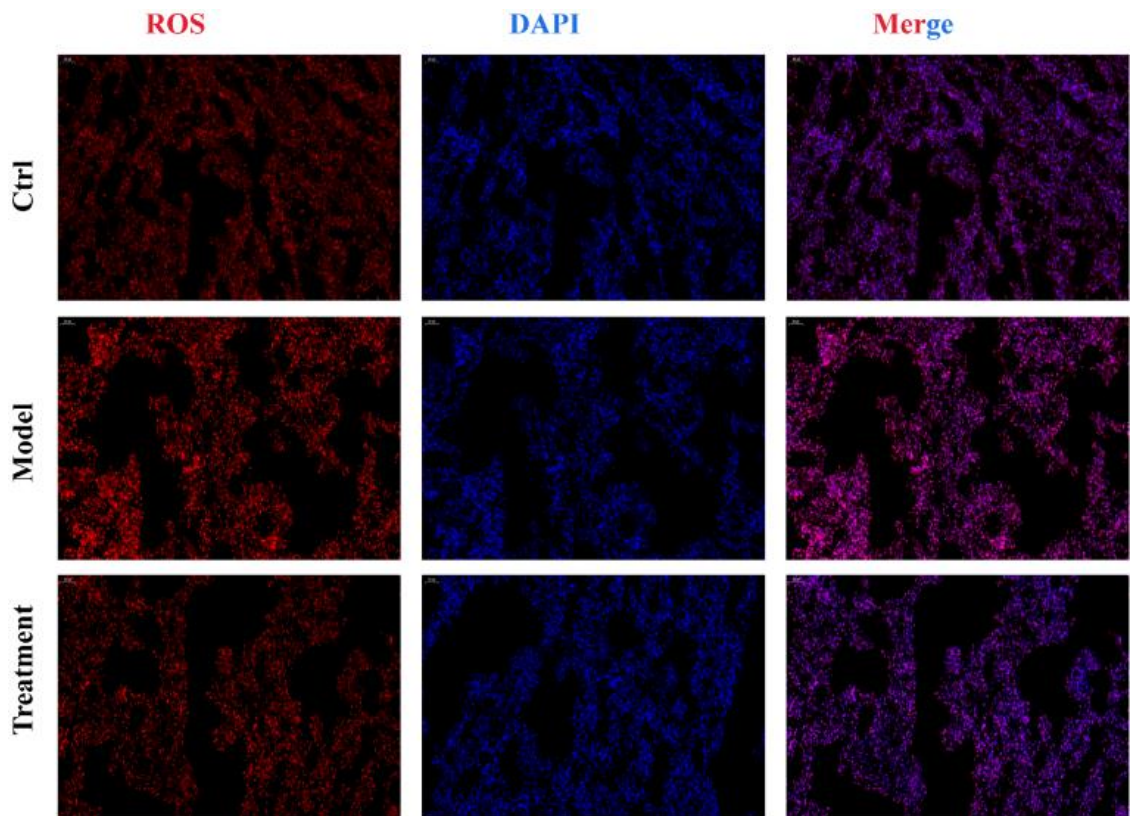


Fig .17 Changes in ROS level after BMMSC treatment (200 ×) (n=5, #P <0.001 compared with the control group, ***P <0.001 compared with the model group)

To explain the regulatory effect of BMMSC on aging-related inflammation, the levels of IL-1 β , IL-17A, and TNF- α were detected by ELISA. IL-1 β was found to be significantly decreased in blood serum (P <0.05) compared with the model group at 30 and 60 days after BMMSC treatment and returned to the original levels after 90 days. Besides, TNF- α was found to be significantly decreased (TNF- α) after 30 days (P <0.05), and returned to original levels after 60 days, and remained unchanged. There was no significant change in IL-17A levels (Fig .18A).

The changes in the levels of inflammatory factors including IL-1 β , IL-6, TNF- α , and IL-10 in the lung after BMMSC treatment were determined by western blot analysis. The levels of IL-1 β , IL-6, TNF- α in the treatment group were significantly lower than in the model group. The level of IL-10 in model group was significantly lower than in the control group (P <0.05), but was significantly increased after BMMSC treatment (Fig .18B), (P <0.05).

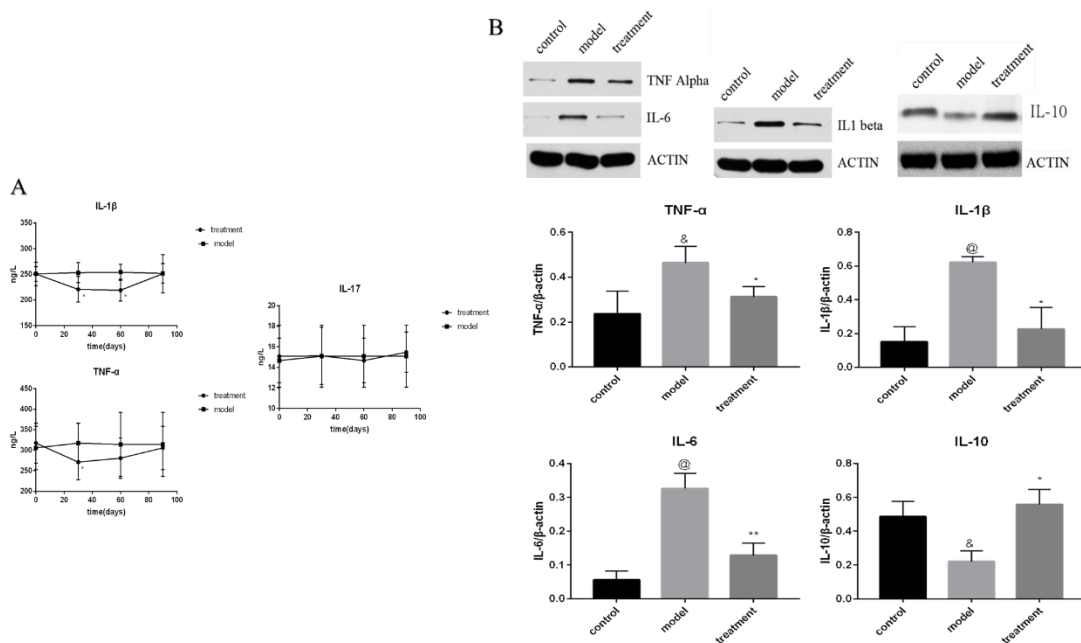
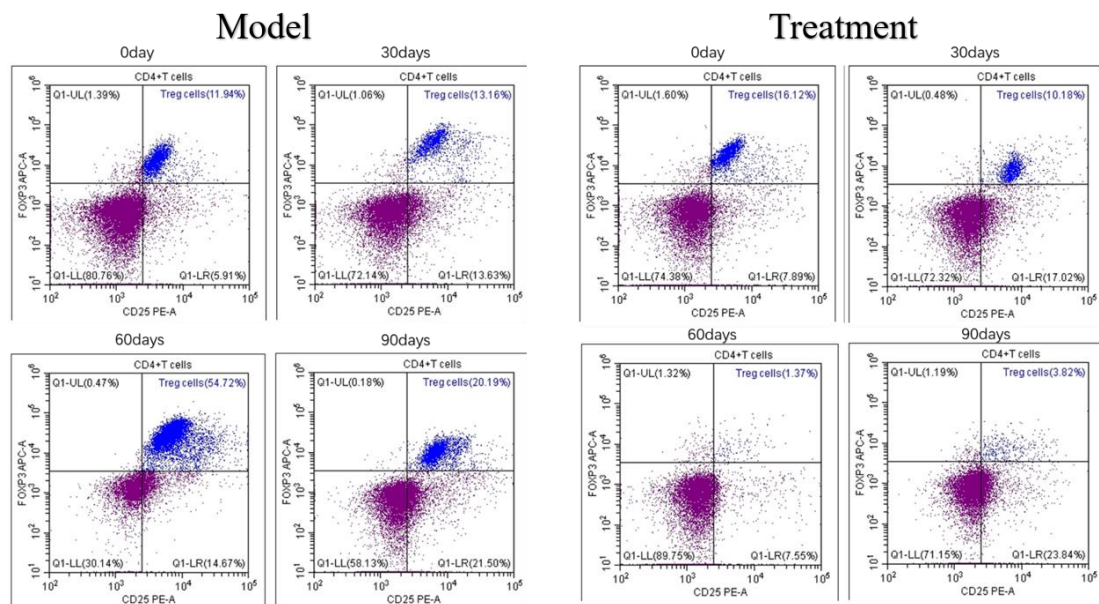


Fig .18 Changes in the inflammatory factors in the lung tissue after BMMSC treatment **a.** Changes in the level of inflammatory factors in peripheral blood after cell therapy (n=5, *P <0.05 compared with the model) **b.** Changes in inflammatory factors in lung tissue after BMMSC treatment (n=5, *P <0.05 compared with the model)

group, ** P <0.01 compared with the model group, & P <0.05 compared with the control group, @P <0.001 compared with the control group).

Effect of BMMSC treatment on immune regulatory cells

As described above, there were observed changes in the expression levels of inflammatory factors in peripheral blood and lung tissue after BMMSC treatment. Treg cells are a class of cells with immune-regulatory functions and also play a vital role in the regulation of inflammation. The ratio of Treg cells in the peripheral blood was measured by flow cytometry. The results showed that the Treg ratio in macaque peripheral blood decreased significantly at 30 days after BMMSC treatment (P <0.01), and reached its minimum at 60 days after treatment (P <0.0001) compared with the model group. However, there was no significant change in the ratio of Treg cells at 60 and 90 days (Fig .19), (P> 0.05).



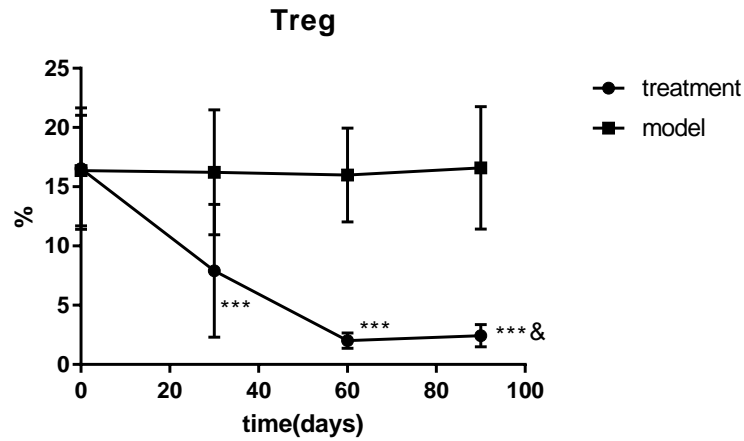


Fig .19 Changes in Treg cell ratio in peripheral blood after BMMSC treatment (n=5, ***P <0.001 compared with the model group, & P > 0.05 compared with 60 days after treatment)

To determine whether the changes in Treg cells in the periphery and lung tissue were consistent, the Treg cell surface marker FOXP3 was used and detection was performed by immunohistochemistry. The content of FOXP3 in the lung tissue of the model group was found to be significantly higher compared with the control group (P < 0.01). Besides, the content of FOXP3 in the treatment group was significantly lower than that in the model group (P <0.0001), and the control group (Fig .20).

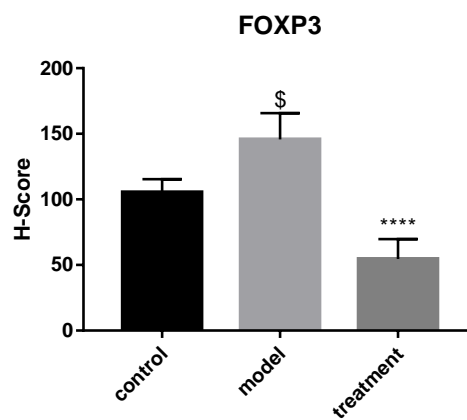
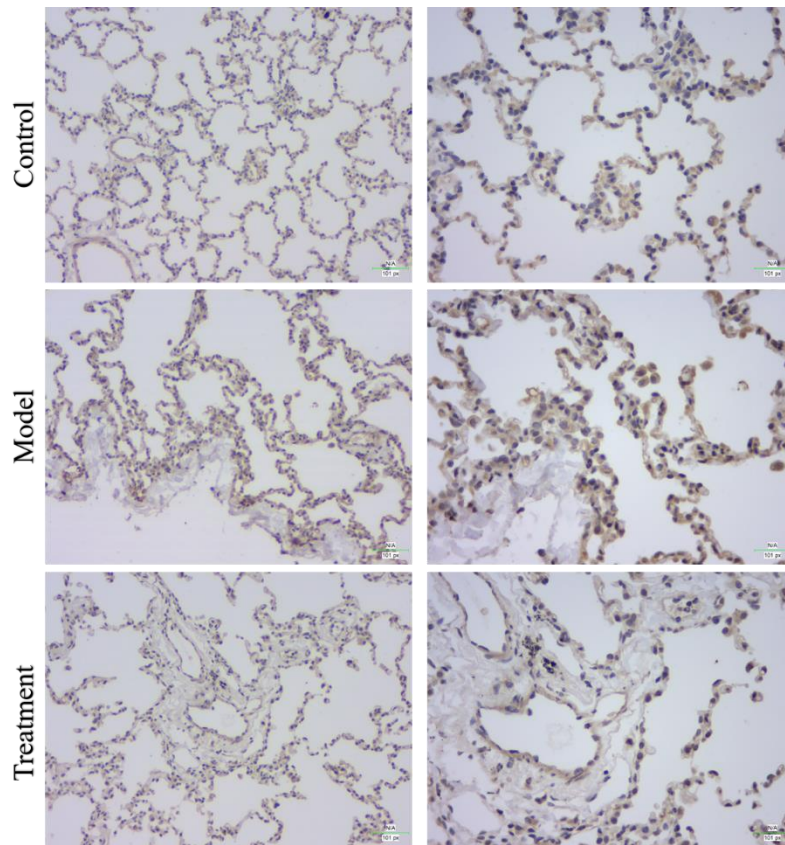


Fig .20 Changes in FOXP3 content in the lung tissue after BMMSC treatment (n=5, ****P < 0.0001 compared with the model group, \$ *P < 0.001 compared with the control group).

Discussion

Changes in lung tissue structure associated with aging, are characterized by enlarged alveoli, damaged alveolar walls, decreased gas exchange surface area, increased airway obstruction or occlusion, decreased pulmonary vascular density,

deepened fibrosis, and decreased elastin content ^[1]. In this study, we observed these phenomena through pathological analysis. Besides, the changes in the lungs were detected by PET-CT, which revealed a significant increase in light transmittance (CT value) in lung tissue after BMMSC treatment. However, a significant decrease in SUV max values and fibrosis were observed. Masson staining revealed that collagen deposition in the treatment group was significantly reduced compared to the model group. Immunohistochemistry analysis showed that alveolar vascular density in the treatment group was significantly increased compared to the model group. However, HE staining showed no significant reduction in alveolar size, which was inconsistent with the results of PET-CT and results reported in other previous studies on mesenchymal stem cells in the treatment of COPD ^[20-22]. Breathing is a dynamic process, and changes in the tissues around the alveoli determine the lung's inspiratory function and Alveolar size. Due to changes in the air in the lungs during inspiration and expiration, PET-CT or HE staining may not sufficiently evaluate whether BMMSC can repair the deterioration of alveolar size during actual respiration in elderly lung tissue. Therefore, to assess the beneficial effects of BMMSC, observation should be performed from multiple directions.

SA- β -gal is a hydrolase enzyme that catalyzes the hydrolysis of β -galactosides into monosaccharides only in senescent cells. P53 and its downstream gene P21 and TCAB1, have been associated with the control of cellular aging ^[13, 15].

In this study, type II alveolar epithelium cells (A549 cells) were used, and aging was induced by hydrogen peroxide. Following co-culture with BMMSC, β -galactoside staining, RT-PCR, and flow cytometry were used to determine the changes in β -galactosidase, P53, P21, and TCAB1 expression levels as well as the oxidative stress levels, apoptosis, and proliferation in A549 cells. The results confirmed that BMMSC can reverse the aging-related characteristics of type II alveolar epithelial cells (A549 cells). These results were consistent with those reported in our previous study on the effect of bone marrow mesenchymal stem cells on the 293T cell senescence model ^[13]. Besides, we used proSPC to label type II alveolar epithelial cells, and determine the

number by immunofluorescence. The results showed that the number of type II alveolar epithelial cells in the treatment group was significantly higher than that in the model group. To some extent, these results were consistent with the *in vitro* experiments.

High inflammation and oxidative stress are important factors driving degeneration of tissues and organs during aging [6, 15, 23]. In this study, we found high level of age-related inflammation and oxidative stress in elderly macaque. Besides, the expression of inflammatory factors TNF- α , IL-1 β , and IL-17A in the peripheral blood was analyzed after 30, 60 and 90 days after BMMSC treatment. After 180 days histological and ROS level analysis was performed and the results showed that the serum IL-1 β level was significantly reduced 30 days after BMMSC treatment, but the level returned to normal at 60 and 90 days. However, western blot analysis of the lung tissue, showed that IL-1 β remained relatively lower than in the model group after 6 months of treatment. Furthermore, TNF- α expression levels appeared to be inconsistent in the lungs and peripheral blood. The content of TNF- α in the peripheral blood decreased significantly after 30 days of cell transfusion and returned to the levels before treatment at 60 and 90 days. However, after 6 months, western blot analysis of the lung tissue, found that TNF- α expression levels were significantly lower than in the model group. This inconsistency between the circulation and lung tissue expression levels differed from that reported in previous studies on rodent lung injury models [24, 25]. Besides, our results show that IL-6 was downregulated in the lung tissue compared to the model group after BMMSC treatment. Therefore, mesenchymal stem cells, such as BMMSC, have a regenerative effect in the aging lung tissue of macaque.

Treg cells play an important role in the control of the immune response. Specifically, they play a central role in immune homeostasis and in preventing autoimmunity. They are produced by the thymus and lymph and exported to the entire body, where they inhibit the activation and proliferation of potential self-reactive T cells, thereby regulating the body's immunity and inflammation. Some studies have found that the number and function of Treg cells change significantly in the aging body. ZHAO et al reported that the ratio of Treg cells in the CD4 + cells of

peripheral blood in elderly mice, was significantly increased and the function was significantly reduced [26]. IL-10 is a multi-functional cytokine, which regulates the growth and differentiation of cells, participates in inflammatory reactions and immune responses, and is recognized as an immunomodulatory cytokine used by almost all innate immune cells [27]. Current studies have shown that the number and function of Treg cells have a regulatory effect on CD4⁺ and CD25⁻ cells to activate the release of IL-10. Aging affects the ability of CD4⁺, CD25⁺, FOXP3⁺ T cells to regulate the production of IL-10 [28]. Besides, mesenchymal stem cells, are powerful immune regulatory cells, with not only a regulatory effect on Treg cells but also strongly influence IL-10 production. Some studies have reported that mesenchymal stem cells can increase the production of IL-10 by communicating with macrophages, B lymphocytes, and dendritic cells or by secreting PGE2, IDO, IL-6, and HO-1 [29]. In this study, CD4, CD25, and FOXP3 were used as markers to detect the changes in the ratio of Treg cells in peripheral blood within 90 days after mesenchymal stem cell treatment. Treg cells in peripheral blood were found to continuously decrease from 0 to 60 days after BMMSC treatment, and the low levels were maintained from 60 to 90 days. These results were inconsistent with those reported in previous studies on the regulation of Treg cells by mesenchymal stem cells under extremely high inflammatory conditions [29]. Therefore, it was not clear whether BMMSC regulated the entry of Treg cells into the tissues, hence reducing the Treg ratio in peripheral blood. Therefore, FOXP3 was used as a marker to further explore the level of Treg cells in the lung tissue. However, the findings from the lung tissues were consistent with those in the peripheral blood, but the FOXP3 levels in the lung tissue of the treatment group were significantly reduced. Therefore, this was speculated to be related to the extremely high inflammation levels, and the mesenchymal stem cells are not sufficient enough to adjust the inflammation level to a normal state and thus requires more Treg cells to be mobilized to deal with the extremely high inflammation. However, under normal aging conditions, the body's inflammation is not very high and can be well controlled by mesenchymal stem cells, which may not require too many Treg cells to be mobilized. This therefore, leads to reduced Treg levels. The content of IL-10 in the lung tissue was

detected by western blot analysis. The results showed that after 6 months of BMMSC treatment, the content of IL-10 in the lung tissue of macaque was significantly higher than that of the model group. These findings were consistent with the short-term observation in a previous mesenchymal stem cell treatment model of lung injury [30]. However, the decrease in the ratio of Treg cells was inconsistent with the phenomenon of elevated IL-10, and this shows that BMMSC treatment can promote the secretion of IL-10 through other mechanisms not related to Treg.

In summary, this study reveals for the first time that BMMSC delays aging-related lung degeneration in the elderly macaque. This study had limitations. Due to experimental limitations, the impact of BMMSC on lung function was not explored in this study. Besides, the mechanisms by which BMMSC improved lung degeneration was also not explored.

Conclusions

1. Obtaining elderly model of pulmonary degenerative macaque shows that the alveolar cavity is enlarged, the structure of the lung is disordered, the pigmentation is increased, the degree of fibrosis is increased, and the capillary density is decreased.

2. BMMSC can reduce the degree of pulmonary fibrosis in elderly macaques, reduce the level of inflammation in the lung and peripheral blood, increase the expression of VEGF in lung tissue, increase the density of capillaries around the alveoli, and reduce the content of Treg cells in peripheral blood and lung tissue.

3. BMMSC can reduce the expression of type II alveolar epithelial aging-related genes, reduce its apoptosis and oxidative stress levels, and promote proliferation. BMMSC can increase the number of type II alveolar epithelium in lung tissue.

Declarations

- **Ethics approval and consent to participate**

Experimental protocols were approved by the Experimental Animal Ethics Committee of the 920th Hospital of the PLA Joint Logistics Support Force.

- **Consent for publication**

Not applicable.

- **Availability of data and material**

All data generated or analysed during this study are included in this published article.

- **Competing interests**

The authors declare that they have no competing interests.

- **Funding**

This work was supported by grants from the Yunnan Science and Technology Plan Project Major Science and Technology Project (2018ZF007), the Yunnan Fundamental Research Projects (2017FB042)

Authors' contributions

YKY,XQZ,YL and YYW made substantial contributions to study conception and design, data acquisition, or data analysis and interpretation.

YKY and RGP agree to be accountable for all aspects of the work and ensure that questions related to the accuracy or integrity of any part of the work will be appropriately investigated and resolved.

XHP and XQZ have given final approval of this version of the manuscript for publication.

XQZ, XHP, HYH, YKY and RQP have been involved in drafting the manuscript or revising it critically for important intellectual content.

All authors read and approved the final manuscript.

- **Acknowledgements**

We thank Freescience's Experts for assisting with the preparation of this manuscript.

Reference

[1] TRAN D, RAJWANI K, BERLIN D A. Pulmonary effects of aging [J]. Current Opinion in Anesthesiology, 2017, 31(1): 1.

- [2] VERBEKEN E K, CAUBERGHES M, MERTENS I, et al. The senile lung. Comparison with normal and emphysematous lungs. 1. Structural aspects [J]. Chest, 1992, 101(3): 793-9.
- [3] TURNER J M, MEAD J, WOHL M E. Elasticity of human lungs in relation to age [J]. Journal of applied physiology, 1968, 25(6): 664-71.
- [4] LOWERY E M, BRUBAKER A L, KUHLMANN E, et al. The aging lung [J]. Clinical interventions in aging, 2013, 8(1489-96).
- [5] SKLOOT G S. The Effects of Aging on Lung Structure and Function [J]. Clinics in geriatric medicine, 2017, 33(4): 447-57.
- [6] MEINERS S, EICKELBERG O, KONIGSHOFF M. Hallmarks of the ageing lung [J]. The European respiratory journal, 2015, 45(3): 807-27.
- [7] XI J, YAN X, ZHOU J, et al. Mesenchymal stem cells in tissue repairing and regeneration: Progress and future [J]. Burns Trauma, 2013, 1(1): 13-20.
- [8] KENNETH S, YERKOVICH S T, CHAMBERS D C. Mesenchymal stem cells and the lung [J]. Respiriology, 2013, 18(3): 397-411.
- [9] CUI P, XIN H, YAO Y, et al. Human amnion-derived mesenchymal stem cells alleviate lung injury induced by white smoke inhalation in rats [J]. Stem Cell Res Ther, 2018, 9(1): 101.
- [10] RUBIO G A, ELLIOT S J, WIKRAMANAYAKE T C, et al. Mesenchymal stromal cells prevent bleomycin-induced lung and skin fibrosis in aged mice and restore wound healing [J]. Journal of cellular physiology, 2018, 233(8): 5503-12.
- [11] SATO K, OIWA R, KUMITA W, et al. Generation of a Nonhuman Primate Model of Severe Combined Immunodeficiency Using Highly Efficient Genome Editing [J]. Cell stem cell, 2016, 19(1): 127-38.
- [12] GIBBS R A, ROGERS J, KATZE M G, et al. Evolutionary and biomedical insights from the rhesus macaque genome [J]. Science (New York, NY), 2007, 316(5822): 222-

34.

[13]PAN X H, CHEN Y H, YANG Y K, et al. Relationship between senescence in macaques and bone marrow mesenchymal stem cells and the molecular mechanism [J]. *Aging*, 2019, 11(2): 590-614.

[14]BARNES P J. Inflammatory mechanisms in patients with chronic obstructive pulmonary disease [J]. *J Allergy Clin Immunol*, 2016, 138(1): 16-27.

[15]LOPEZ-OTIN C, BLASCO M A, PARTRIDGE L, et al. The hallmarks of aging [J]. *Cell*, 2013, 153(6): 1194-217.

[16]ROTTENBERG H, HOEK J B. The path from mitochondrial ROS to aging runs through the mitochondrial permeability transition pore [J]. *Aging cell*,

[17]MONICA DE LA FUENTE J M. An Update of the Oxidation-Inflammation Theory of Aging: The Involvement of the Immune System in Oxi-Inflamm-Aging [J]. *Current Pharmaceutical Design*, 15(26): p.3003-26.

[18]PALIWAL S, CHAUDHURI R, AGRAWAL A, et al. Regenerative abilities of mesenchymal stem cells through mitochondrial transfer [J]. *Journal of Biomedical Science*, 25(1): 31.

[19]HARRELL C R, SADIKOT R T, PASCUAL J, et al. Mesenchymal Stem Cell-Based Therapy of Inflammatory Lung Diseases: Current Understanding and Future Perspectives [J]. *Stem Cells International*, 2019, 2019(4236973)-.

[20]FIKRY E M, SAFAR M M, HASAN W A, et al. Bone Marrow and Adipose-Derived Mesenchymal Stem Cells Alleviate Methotrexate-Induced Pulmonary Fibrosis in Rat: Comparison with Dexamethasone [J]. *Journal of biochemical and molecular toxicology*, 2015, 29(7): 321-9.

[21]WECHT S, ROJAS M. Mesenchymal stem cells in the treatment of chronic lung disease [J]. *Respirology*,

[22]HUANG K, KANG X, WANG X, et al. Conversion of bone marrow mesenchymal

stem cells into type II alveolar epithelial cells reduces pulmonary fibrosis by decreasing oxidative stress in rats [J]. *Molecular medicine reports*, 2015, 11(3): 1685-92.

[23]MURRAY M A, CHOTIRMALL S H. The Impact of Immunosenescence on Pulmonary Disease [J]. *Mediators Inflamm*, 2015(1-10).

[24]GUPTA N, SU X, POPOV B, et al. Intrapulmonary Delivery of Bone Marrow-Derived Mesenchymal Stem Cells Improves Survival and Attenuates Endotoxin-Induced Acute Lung Injury in Mice [J]. *Journal of Immunology*, 179(3): 1855-63.

[25]MEI S H J, MCCARTER S D, DENG Y, et al. Prevention of LPS-Induced Acute Lung Injury in Mice by Mesenchymal Stem Cells Overexpressing Angiopoietin 1 [J]. *PLoS medicine*, 4(9): e269.

[26]ZHAO L, SUN L, WANG H, et al. Changes of CD4+CD25+Foxp3+ regulatory T cells in aged Balb/c mice [J]. *J Leukoc Biol*, 81(6): 1386-94.

[27]GABRYŠOVÁ L, HOWES A, SARAIVA M, et al. The Regulation of IL-10 Expression [J]. *Current Topics in Microbiology & Immunology*, 2014, 380(157-90).

[28]HWANG K A, KIM H-R, KANG I. Aging and human CD4+ regulatory T cells [J]. *130(8): 509-17.*

[29]NAJAR M, RAICEVIC G, FAYYAD-KAZAN H, et al. Mesenchymal stromal cells and immunomodulation: A gathering of regulatory immune cells [J]. *Cytotherapy*, 18(2): 160-71.

[30]Activation of Human Mesenchymal Stem Cells Impacts Their Therapeutic Abilities in Lung Injury by Increasing Interleukin (IL)-10 and IL-1RN Levels [J]. *Stem cells translational medicine*,